J Am Oil Chem Soc (2010) 87:1115–1125
DOI 10.1007/s11746-010-1596-8

ORIGINAL PAPER

Pre-Nucleation Structuring of TAG Melts Revealed by Fluorescence Polarization Spectroscopy and Molecular Mechanics Simulations

E. Dibildox-Alvarado · T. Laredo · J. F. Toro-Vazquez · A. G. Marangoni

Received: 17 February 2010 / Revised: 8 April 2010 / Accepted: 22 April 2010 / Published online: 13 May 2010

Abstract We have studied the pre-nucleation behavior of tripalmitin (TP) and tristearin (TS) in blends with triolein (TO), high oleic safflower oil (HOSfO) and soybean oil (SBO) by means of fluorescence polarization spectroscopy (FPS) and molecular mechanics simulations (MM). The FPS measurements at different temperatures showed that there is an increase in the anisotropy of the TP:HOSfO and TP:SBO blends as opposed to the TP:TO sample. This increase is directly related to an increase in the microviscosity of the blend which is interpreted as a structuring step prior to the nucleation and growth of the crystals. A similar but less pronounced effect was also observed in the TS:SBO blends. We performed MM simulations in an attempt to understand the molecular interactions responsible for this behavior. The simulation results have shown that short range van der Waals (vdW) interactions are the ones responsible for the increase in the microviscosity of the blends prior to crystallization. Our results also indicate that the presence of molecules that contain at least one chain of palmitic acid in their triglyceride (TAG) composition will induce a pre-nucleation increase in the microviscosity of the blend in both TP and TS containing systems. Lastly, we studied the applicability of these conclusions to longer chain TAG analogues. Our MM results show that hypothetical blends of TS and TAGs containing stearic acid in their structure, will not have a low enough vdW energy to account for an increase in the microviscosity. Hence, there seems to be a specific interaction particularly favorable when the oil contains TAGs with at least one palmitic acid chain.

Keywords Triglycerides · Structuring · Pre-nucleation · Fluorescence polarization spectroscopy · Molecular mechanics

E. Dibildox-Alvarado · J. F. Toro-Vazquez
Facultad de Ciencias Quimicas, Universidad Autonoma de San Luis Potosi, San Luis Potosi, Mexico

E. Dibildox-Alvarado
Universidad Autonoma de Queretaro, DIPA-PROPAC, Querétaro, Mexico

T. Laredo · A. G. Marangoni (✉)
Department of Food Science, University of Guelph, Guelph, Canada
e-mail: amarango@uoguelph.ca

Introduction

In principle all liquids are isotropic: the molecular motions within the fluid are Brownian in nature and can be described by the Stokes–Einstein relationship. However, under certain circumstances a fluid may display a preferential motion or have an orientational restriction. It is then said that the fluid is structured and hence displays anisotropy [1]. Examples of these structured liquids are liquid crystalline (LC) polymers. The state of their solution (lyotropic) or melt (thermotropic) is between the boundaries of solid crystals and isotropic liquids. This state is also referred to as a mesomorphic structure or a mesophase. The anisotropic optical properties of liquid crystal polymeric fluids are like those of regular solids, but their molecules are free to move similar to liquids. One of the many interesting properties of these mesogenic structures is that they show spontaneous anisotropy and are easily oriented, provided that they are in a LC state. This is an extremely useful property because a high degree of molecular alignment in the fluid state can determine the properties of the solidified end product. This is essential,

for example, for making high stiffness materials such as Kevlar (DuPont), Vectra (Hoechst Celanese) and Xydar (Amoco) among other classical examples.

It has been suggested that triacylglycerides (TAGs) also display anisotropy when in the LC state. The phase behavior of TAGs has been the subject of several studies due to the importance of polymorphism in technical fat processing.

Several groups have proposed different molecular arrangements for TAG melts. Namely, nematic and smectic phases have been the two mesophases most argued over on this subject. Cebula et al. [2] have proposed that TAGs in melts arrange themselves in a nematic phase characterized by molecular symmetry axes lined up parallel but without any positional order. Larsson, on the other hand, has postulated that the lipid molecules in the LC state arrange themselves in a lamellar-type of order typical of a smectic phase, where the molecules posses some positional order [3]. Sato and co-workers [4, 5] have shown through synchrotron radiation X-ray diffraction that TAGs in which one of the chains is unsaturated, display a LC phase characterized by lamellar ordering. However, their results are for pure TAGs that were quenched to temperatures well below the corresponding melting point and then heated rapidly to the target temperature. More recently, Corkery et al. [6] have proposed that molten TAGs form a discotic phase in which the triglyceride molecules exist in the liquid state with fully splayed chains, approximating "Y''-shapes. Regardless of the actual mesophase, all the work mentioned above agrees on the fact that, TAG molecules are somehow structured in a LC-like state [2–9]. However, they all deal with model, single TAG component, samples. Due to the applicability of multicomponent TAG blends in food, cosmetic and pharmaceutical industries, the present work is an attempt to study the structure in the liquid state, prior to nucleation of these more complex systems. Our systems are meant to provide different degrees of molecular compatibility between different solvent phases [triolein, safflower oil high in triolein, and soybean oil (SBO)] with the saturated TAGs of interest (tripalmitin and tristearin).

The shape and size of these LC structures changes with the diffusion rate of the molecules [8]. This translates into a change in the viscosity of the system as a function of temperature. Thus, oil viscosity is an indirect measurement of the structure or anisotropy of TAGs in the liquid state. When vegetable oils are cooled, the viscosity increases due to a higher organization of the TAGs [10]. Marangoni has shown that an increase in the anisotropy, as measured by fluorescence polarization, is observed upon cooling of oils, which is correlated to an increased viscosity of the medium [11]. Hence, the combined measurements of viscosity and anisotropy of vegetable oils provide information regarding the liquid structure in a pre-nucleation state and its relationship with crystallization.

Fluorescence polarization is a technique used to study the rotational movement of molecules in suspensions as well as in solutions [12] and provides information about concentration, binding events, and molecular structure, diffusion, mobility on membranes, and structure on surfaces [13, 14]. In fluorescence polarization spectroscopy (FPS), a fluorophore is used as a probe to study the hydrodynamic behavior at the molecular level. Briefly, as the stiff fluorophore molecules in a fluid diffuse throughout the bulk, they undergo a precessional motion characterized by a rotational correlation time, Φ. This is a time constant that characterizes the molecular rate of rotation. When polarized light impinges an ensemble of fluorophores, only those that are aligned with the plane of polarization will be excited. The emission can then undergo two different paths depending on the lifetime of the process: If the fluorescence lifetime of the excited fluorescent probe is much longer than the rotational correlation time of the molecule it is bound to, the molecules will randomize in solution during the process of emission. As a result, the emitted light of the fluorescent probe will be depolarized. If, on the contrary, the fluorescence lifetime of the fluorophore is much shorter than the rotational correlation time, the excited molecules will stay aligned during the process of emission. In this case the emission will be polarized. Hence, the extent of depolarization is a measure the rotational correlation time. Because the molecules experience intermolecular friction forces that oppose their rotational diffusion, the extent of the depolarization is a measure of the anisotropy of the system and, in turn, of its microviscosity. A great deal of theoretical and empirical expressions have been derived for this purpose and the reader is referred to the works of Marangoni [11], Royer [15] and Mann and Krull [16] for a comprehensive review of the technique.

The interactions responsible for an increase in the anisotropy of a fluid are molecular in nature. The knowledge of these interactions can be explored by means of computer simulations. In this work, we have used molecular mechanics (MM) to model the system in order to understand the role of energetics in achieving a particular state. MM is a simple method which describes the energy of the system in terms of a set of classically derived potential functions.

In particular, we evaluate here the liquid structure of binary model systems of TAGs prior to crystallization through MM simulations. Similar studies have been carried out in the past in different systems. For example, Nagarajan and Mayerson [17] have used MM to understand the role of energetics in the formation of the helical conformation of isotactic polypropylene in an attempt to understand

nucleation in the early stages of crystallization. Interestingly, the work of Sato and co-workers [5] on monounsaturated TAGs notes that the ordering sequences between the lamellar stacking and the lateral packing of these molecules is very similar to that found upon crystallization of isotactic polypropylene [18]. Hence, we believe that using MM simulations to study complex TAG blends (e.g. fats) crystallized under non-isothermal conditions, would provide information regarding the energetic interactions responsible for the structuring in the liquid state just before nucleation takes place.

Materials and Methods

Triacylglycerides, Vegetable Oils, and Blend Preparation

Tripalmitin (TP), tristearin (TS), and triolein (TO) with purities higher than 99% were obtained from Sigma Chemical Co. (St. Louis, MO). Refined, bleached and deodorized high oleic safflower (HOSfO) and SBO were obtained from local manufacturers. TAG composition of the oils was determined by HPLC following the procedure described by Perez-Martinez et al. [19] The composition of major TAGS was reported as the mean (±standard deviation) of at least three independent measurements. Each of the saturated TP and TS were blended with either TO, HOSfO, or SBO in a 25:75 (wt:wt) ratio. After 20 min at 80 °C with constant gentle stirring, the blends were stored under nitrogen atmosphere at 2 °C in amber glass vials.

DSC Measurements

The crystallization and melting thermograms of the blends were obtained by DSC using a TA Instruments Model Q2000 (TA Instruments, New Castle, DE, USA). After calibration of the equipment, blend samples (6–8 mg) were sealed in aluminum pans, heated at 80 °C for 20 min and then cooled to −60 °C at a rate of 10 °C/min. After 2 min at this temperature the samples were heated to 80 °C at a rate of 5 °C/min. In all cases an empty pan was used as reference. The melting temperature (T_m) and enthalpies were calculated from the melting thermograms using the equipment software.

X-Ray Diffraction

X-ray diffraction patterns of the crystallized blends (14 mg) were obtained using a Rigaku Multiplex Powder X-ray diffractometer (Rigaku, Japan) using a Cu source X-ray tube ($\lambda = 0.1542$ nm) at 40 kV and 44 mA. After crystallizing the blend at the corresponding temperature using a cooling rate of 10 °C/min, the X-ray diffraction was recorded at scanning rate of 1° per min from 1° to 30° 2θ. The temperature was controlled with a Peltier system and the results were analyzed using MDI's Jade 6.5 software (Rigaku, Japan).

Viscosity Measurements

The viscosity of the blends investigated was obtained at different temperatures with a mechanical spectrometer (Physica MCR 301, Anton Paar, Stuttgart, Germany) equipped with TruGap system (P-PTD200/TG) using a 2.5-cm diameter parallel-plate geometry (PP25/TG). The temperature was controlled by a Peltier system located in both the base and top of the measurement geometry through a Peltier-controlled hood (H-PTD 200). The control of the equipment was made through the software Start Rheoplus/32 version 2.65 (Anton Paar, Graz-Austria). After 20 min at 80 °C the system was cooled at a rate of 10 °C/min. At each 5 °C interval during the cooling stage, the shear stress was determined by applying a logarithmic shear rate sweep from 1 to 100 per s. Before the measurements the system was allowed to achieve temperature equilibrium for 5 min. The viscosity (η) was determined as the slope of shear stress versus shear rate by linear regression. Two independent determinations were obtained for each temperature.

Anisotropy Measurements, During the Cooling Stage, Under Isothermal Crystallization Conditions

The anisotropy (r_s) of the blends was calculated using the fluorescence intensities of blends previously labeled with a 1 mM of 1,6-diphenyl-1,3,5-hexatriene (DPH, Sigma, St. Louis, MO, USA) solution in tetrahydrofuran (2 μl/ml). The intensities were measured with a polarizer spectrophotometer (MD-5020 of Photon Technology International, London, Ontario, Canada) equipped with a high speed random access monochromator DeltaRAM using the FeliX32 software. The prefixed wavelength was 360 nm for excitation and 465 nm for emission. The fluorescence intensities of the blends (250 μl samples) were obtained during the cooling (i.e. as a function of temperature) and the isothermal stages (i.e. as a function of time) with the observation polarizer parallel or perpendicular to the incident plane-polarized light. The two intensities were obtained in independent experiments under the same time–temperature conditions. In each case two independent determinations were carried out. For the TP blends, the anisotropy was measured every degree from 36 to 41 °C, and for the TS blends every degree from 46 to 51 °C. Although the range of temperatures is different for the TP and TS blends, the supersaturation conditions are very

similar. The supersaturation ($\ln\beta$) of the melts was calculated as

$$\ln \beta = \frac{\Delta H}{RTT_{\mathrm{m}}}\Delta T \quad (1)$$

where R is the gas constant, T the isothermal crystallization temperature. ΔH the enthalpy of fusion, T_{m} the melting temperature for either TP or TS, and ΔT is the difference between the melting temperature and the temperature of the experimental run [20]. For the anisotropy experiments, $\ln\beta$ ranges from 0.16 to 0.25 and from 0.15 to 0.24 for the TP and TS blends respectively. These ranges indicate that all samples had similar supersaturation conditions.

Temperature control was achieved with a Peltier system attached to a four position cuvette holder (Turret 400, Quantum Northwest). The anisotropy value (r_{s}) was calculated under the cooling and isothermal stages of the blend crystallization considering the G correction for light scattering as described by Lakowicz [21]. The G correction factors for the TP blends were 1.06, 1.02, and 0.97 for TO, HOSfO, and SBO, respectively; and 1.09, 1.03 and 0.96 for the TS blends with TO, HOSfO, and SBO, respectively.

Construction of the MM Initial Configuration

The general considerations to develop these TAGs lamellar structures used the following criteria:

- Saturated TAGs molecules had to be stackable in a chair-like conformation with parallel hydrocarbon chains at positions *sn*-1 and *sn*-3 and anti-parallel at *sn*-2 with a thickness of $2L$. Due to the unsaturation present in oleic acid this was more complicated in the case of triolein (TO) than for the fully saturated TP, and even more so for TAGs having different acyl chains such as PLL or PLO.
- For unsaturated TAGs two possible conformations were explored, such that the hydrocarbon chains at positions *sn*-1 and *sn*-3 were pointing (a) in the same direction as the *sn*-2 chain, and (b) away from the hydrocarbon chain at *sn*-2 position.
- All unsaturations were in *cis* conformation
- Changes in the average tilt angle of the TAGs packing for the three major polymorphs, α, β' and β, had no effect on the energy minimization procedure.

Once these requirements were fulfilled, the actual initial configuration was found such that changes in dihedral angles of each TAG in a stack of four molecules led to a very similar minimization energy. This was taken as an indication of a minimum energy configuration. It should be noted that the vdW energy falls off as r^{-6}, but it can be cut off at much shorter distances. In this work, a cutoff value of 10 Å was used throughout, which increased the speed of the computation significantly.

All the simulations were performed with CS Chem3D Pro (CambridgeSoft v. 3.5.1), 16 molecules were used, stacked in 4 rows of 4 molecules, as shown in Fig. 1. The packing was such that the van der Waals radii of the atoms of adjacent molecules were just in contact with each other. The rows were arranged in both alternating and "sandwiched" conformation. In the latter, two rows of the same molecule were in between two rows of the other molecule. The final result of the energy minimization for these two types of conformation was statistically determined to be equivalent. Hence we used these to calculate an average of 4–6 sets for different mixes of TAGs.

Mixtures of more than two types of TAG proved to be extremely difficult to simulate as the number of variables in the initial configuration increased the uncertainty of the minimization procedure.

Once the initial configuration was set, the MM2 (an all atom force field based on the MM1 functional form [22]) energy minimization was allowed to run until a root mean squared (RMS) gradient value of 0.014 was attained using a steepest descent minimization algorithm. If the slope of the potential energy surface becomes small enough, then the minimization has probably reached a local minimum on the potential energy surface, and the minimization terminates. Our convergence criterion was a good compromise between accuracy and speed of the simulation.

Results

Differential Scanning Calorimetry and X-ray Analysis

DSC measurements were performed on all blends. The melting thermograms (data not shown) consistently showed two endotherms. The lower temperature endotherm is associated with the melting of the TAGs from TO, HOSfO and SBO. The higher temperature endotherm corresponds to the melting of either TP or TS depending on the system. Table 1 summarizes the temperature values for the second endotherm and the corresponding enthalpies of melting as determined from the integration of the peak. It is clear that the fully saturated TAG in each case melts at about the same temperature for the three corresponding blends: about 58 and 65 °C for the TP and TS blends respectively. This is an indication that there are no specific chain–chain interactions between the TP, or TS, and the solvents used in each mixture affecting the solubility and phase behavior of the blends.

The crystallinity of the blends was assessed by X-ray diffraction. Figure 2 shows the X-ray spectra for selected temperatures for both the TP blends (Fig. 2a) and the TS

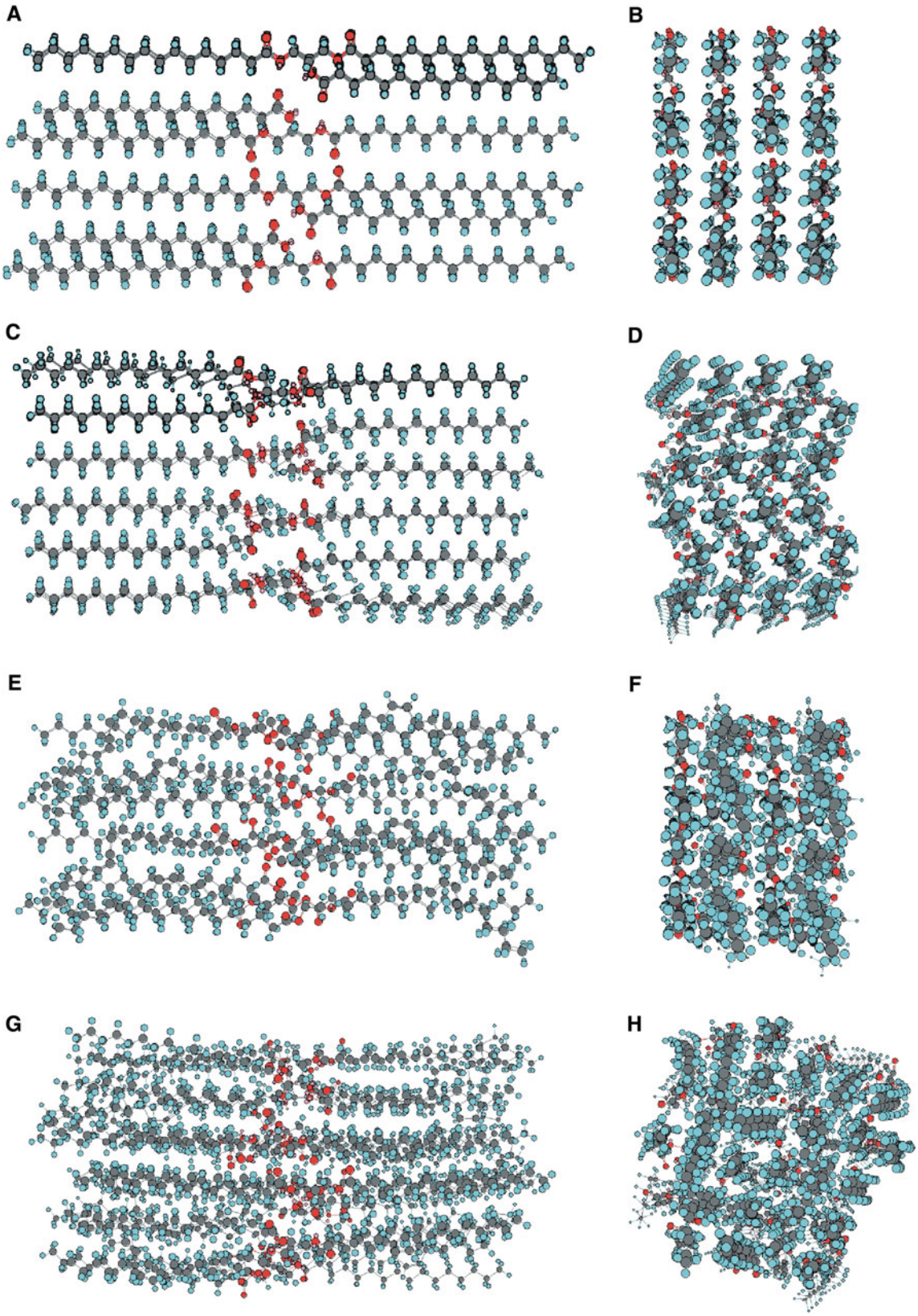

Fig. 1 Stack of 16 molecules arranged in 4 rows of 4 molecules each. **a**–**d** For a TP stack. **e**–**h** For a TP:PLO mix in a 1:1 molecular ratio. The initial configurations are seen from a side (**a**, **e**) and front (**b**, **f**) perspectives. After the energy minimization side (**c**, **g**) and front (**d**, **h**) views are shown for comparison

Table 1 Melting temperatures and enthalpies of fusion for the TP and TS in their respective blends as determined from DSC heating measurements

Blend	T_m (°C)	ΔH (kJ/mol)
TP:TO	57.6 ± 0.4	10.4 ± 0.3
TP:HOSfO	57.5 ± 0.4	10.58 ± 0.2
TP:SBO	57.60 ± 0.01	11.39 ± 0.01
TS:TO	65.17 ± 0.09	11.89 ± 0.01
TS:HOSfO	64.7 ± 0.5	12.8 ± 0.1
TS:SBO	65.0 ± 0.1	12.93 ± 0.01

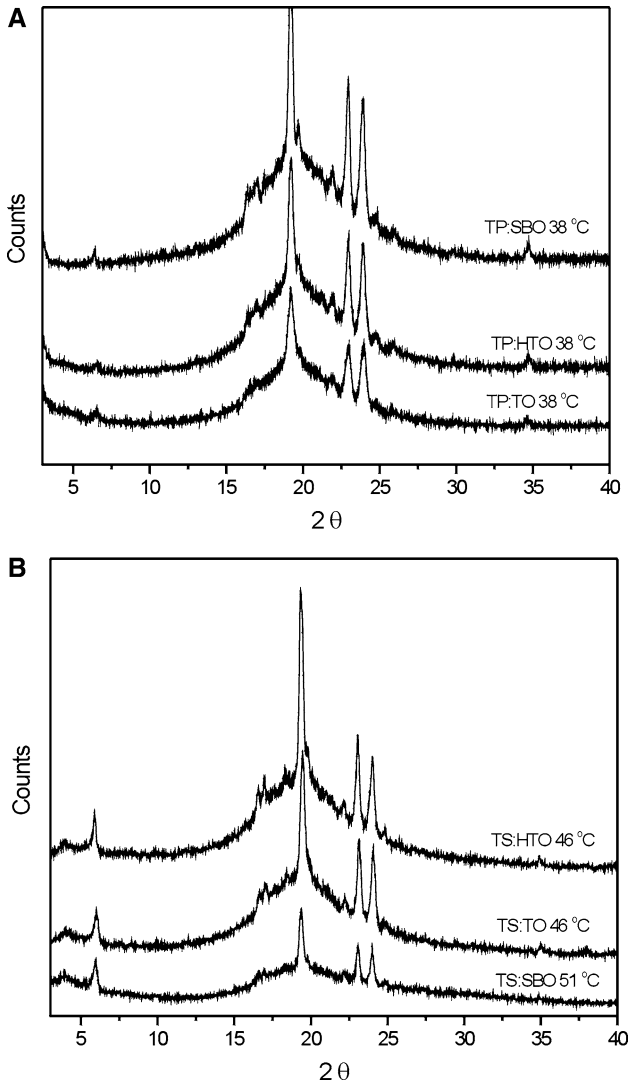

Fig. 2 X-Ray diffraction patterns. All TP blends (**a**) were crystallized at 38 °C. TS blends (**b**) crystallized at 46 or 51 °C as shown in the figure

blends (Fig. 2b). It is clear from the peaks at approximately 19°, 23° and 24° corresponding to spacings of 4.60, 3.85 and 3.70 Å, that the blends crystallized as the β polymorph (triclinic subcell structure).

Fluorescence Polarization Spectroscopy

We have plotted the viscosity of the system determined from rheological measurements as a function of the anisotropy for each of the blends. Table 2 shows the values of slope, intercept and correlation of the linearity for these plots. The high R^2 values clearly indicate that the viscosity and the anisotropy vary linearly, hence showing that the anisotropy, within the range studied, is a measure of the bulk viscosity of the system.

The Perrin equation has been modified by Weber et al. [23] to account for molecules that are not spherical (as is the case for most fluorescent tags), such that:

$$\frac{r_0}{r_s} = 1 + \frac{kT\tau}{\bar{\eta}v_0} \quad (2)$$

where r_s is the molecular anisotropy with r_o/r_s defined as the degree of depolarization, T the absolute temperature, τ the average lifetime of the excited state, k the Boltzmann constant, $\bar{\eta}$ is the microviscosity of the medium, and v_0 the effective volume of the fluorescent probe. The maximum anisotropy value r_o is close to 0.4 for DPH [24]. The van der Waals volume of the DPH probe has been reported to be 233 Å^3 [24]. We have used Eq. 2 to determine the viscosity of the blends and verify the validity of this approach.

Table 3 shows the values of viscosity calculated using the Perrin equation and those determined experimentally for all blends at 55 °C. The fluorescence lifetime, τ, of

Table 2 Slope, intercept and correlation coefficient for plots of viscosity versus anisotropy for the TP (45–80 °C) and TS (55–80 °C) blends

Blend	Slope	y-Intercept ($\times 10^{-3}$)	R^2
TP:TO	0.762	9.4	0.996
TP:HOSfO	0.807	8.3	0.982
TP:SBO	0.674	9.9	0.984
TS:TO	0.719	9.9	0.983
TS:HOSfO	0.852	10.3	0.938
TS:SBO	0.852	9.6	0.972

Table 3 Comparison between the bulk and calculated viscosities using Eq. 2 at 55 °C

Blend	Bulk viscosity η (Pa s)	Microviscosity $\bar{\eta}$ (Pa s)
TP:TO	0.0297	0.0129
TP:HOSfO	0.0301	0.0130
TP:SBO	0.0278	0.0129
TS:TO	0.0310	0.0139
TS:HOSfO	0.0303	0.0119
TS:SBO	0.0294	0.0110

DPH is both temperature and solvent dependent. At 55 °C τ is approximately 10 ns in heavy white paraffin oil [11]. The calculated and experimental viscosities are in the same order of magnitude. However, there is a significant discrepancy between the two. The calculated microviscosity is consistently lower than the experimental values by approximately a factor of 2. The reason could be a physical one, in the sense that the microviscosity could be different than the bulk viscosity of a blend, especially if the fluid is somehow structured. However, this result could also imply that the Perrin equation used here does not really hold for our systems, due to some specific behavior of the blends. Regardless, it is interesting that both sets of values are in the same order of magnitude.

Anisotropy as a Function of Time

Measurements of the normalized anisotropy, $r_s/r_{t=0}$, at different supersaturation conditions are shown in Fig. 3a, b and c for the TP:TO, TP:HOSfO and TP:SBO blends, respectively and in Fig. 3d, e, and g for the TS analogues. All the plots display an initial period of time where the anisotropy is constant. Also, a decrease in the anisotropy at the end of the experiment is common to all measurements due to the scattering of light from newly formed nuclei. In some cases, the anisotropy increases during the course of the experiment before dropping at the end. Within these features, the behavior of the TP and TS blends is different. The time scale of the experiments for the TS samples is on average three times longer (about 20 min) than for the TP blends (between 5 and 7 min). This is an indication of a higher ΔG of nucleation for the TS blends, relative to the TP blends.

The effect of the solvent in TP samples is different in each case. TP:TO blends do not display an increase in the anisotropy at any of the temperatures studied. For the TP:HOSfO and TP:SBO samples, the measurements done at 37, 38 and 40 °C in the former blends and those at all temperatures for the latter one, display a clear increase in the anisotropy. This increase in the anisotropy is related to an increase in the microviscosity of the system and hence is an indication of molecular interactions leading to the structuring of the blend in a pre-nucleation state. The fact that the TP:TO mixes show no increase, clearly implies that the structuring of the fluid is not due to the presence of triolein in the blend. We propose that it must be an effect due to the presence of other TAGs present in the HOSfO and SBO. Furthermore, the peak in anisotropy is highest for the TP:SBO blends, indicating that the strongest ordering effect is in the presence of SBO as the blend solvent.

Several smaller features can be appreciated in Fig. 3. In the measurements of TP:HOSfO at 36 and 38 °C and in those at 46 and 47 °C for the TS:HOSfO mixes, after the initial decrease in anisotropy due to the appearance of crystals, the fluorescence polarization signal becomes very weak and unstable and sometimes a spiking behavior is observed due to artifactual scattering effects. The TAG composition of HOSfO and SBO was determined in our laboratory and it is summarized in Table 4. TAGs present in a concentration of less than 5% in both oils have been omitted from the table for simplicity. Based on our FPS results, the interactions that lead to an increase in the anisotropy are probably related to the presence of TAGs other than TO (OOO in the table) in the blends.

In the case of the TS blends, the general trend is slightly different to that seen in the TP samples. Firstly, the TS:TO samples at 49 and 50 °C show an increase in the anisotropy that it is not seen for any of the TP:TO blends. Secondly, the only increase in anisotropy seen in the TS:HOSfO blends is a spike-like behavior seen at 47 °C. However, the TS:SBO blends display a similar anisotropy increase to the one observed in the TP:SBO mixes if only for the higher temperature experiments. We believe that the increases seen in the TS:TO and TS:HOSfO blends are due to artifacts and hence, are not representative of the behavior of the blend, especially since they occur in the middle of the temperature range. As a consequence, the only blends that display some pre-nucleation ordering for the TS fat are those dissolved in SBO. This is again an indication that there is a TAG-specific interaction at the molecular level responsible for the structuring of the blend prior to crystallization. We could hypothesize that somehow the presence of one or several TAGs present in SBO induces this ordering effect of the fluid and that, if at all present, the concentration is not sufficiently high in the TS:HOSfO blends to allow for the structuring effect. However our results so far, do not allow for a better insight on the forces and conditions necessary for this pre-nucleation increase in the anisotropy to occur. We have used MM simulations to address this aspect.

Molecular Mechanics Simulations

We have performed MM simulations in an attempt to understand the molecular interactions responsible for the experimental behavior seen in the anisotropy measurements of the blends. The energies given by the Chem3D program are divided into bonded and non-bonded interaction energies. The latter one is further divided into Dipole/dipole, long and short range van der Waals interactions. Of these terms, only the short range van der Waals component showed a consistent trend in the results within the reproducibility of the method. The total energy and all other components given as a result of the minimization showed

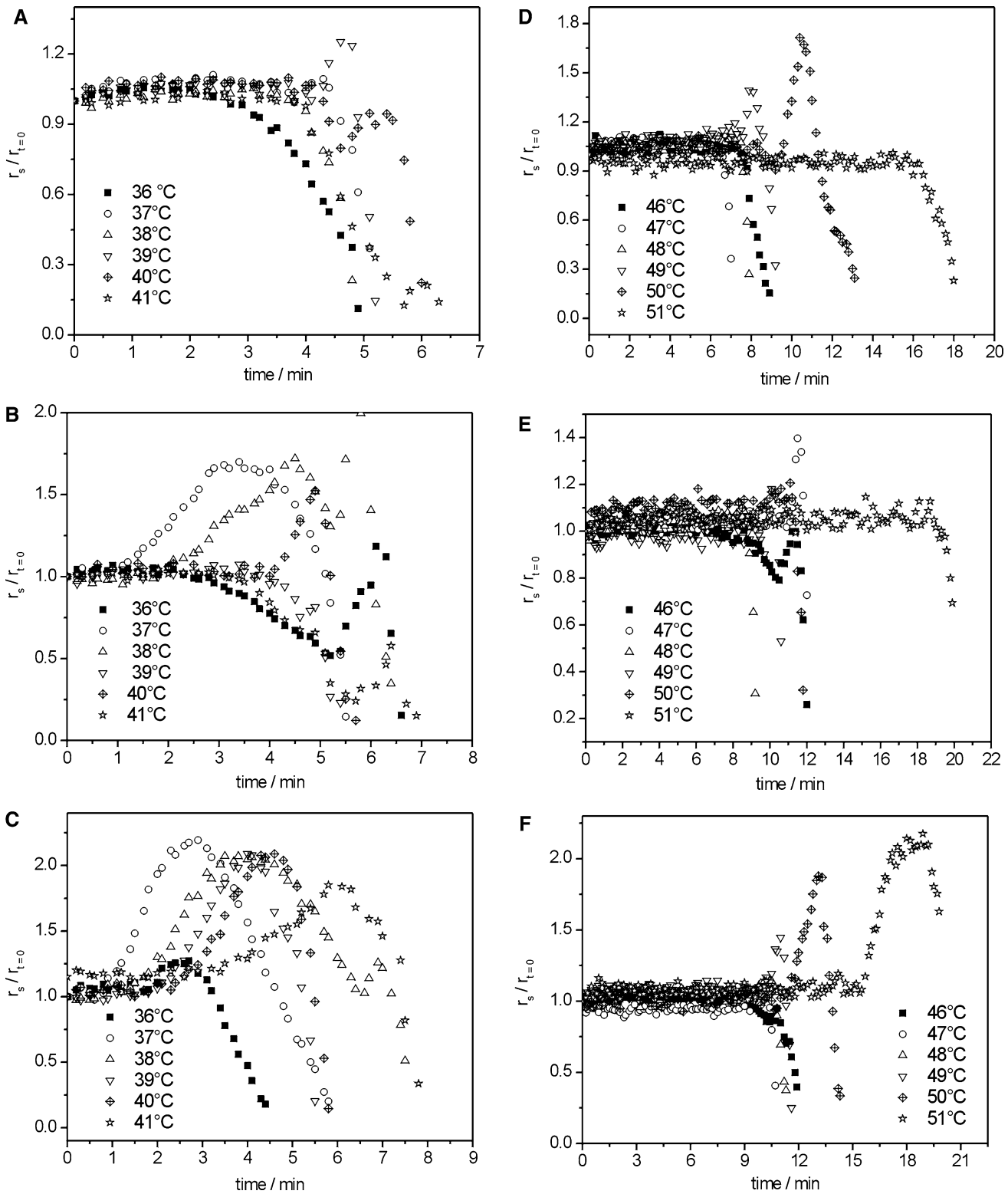

Fig. 3 Normalized anisotropy as a function of time for **a** TP:TO, **b** TP:HOSfO, **c** TP:SBO, **d** TS:TO, **e** TS:HOSfO and **f** TS:SBO at the temperatures indicated in each figure

no particular trend as a function of the type of molecule used. Hence, we refer hereon only to the short range vdW energy in order to explain our experimental results.

The vdW component of a pure TP system upon minimization was determined to be 695 ± 4 kcal/mol. In contrast, a simulation of pure TO resulted in a value of

Table 4 TAG composition (%w/w) of safflower oil high in triolein (HOSfO) and soybean oil (SBO)

TAG	HOSfO	SBO
LLL	0.48 (0.05)	21.4 (0.5)
LLO OLL	2.24 (0.06)	21.2 (0.9)
LLP	0.26 (0.02)	14.5 (0.6)
LOO	16.20 (0.08)	9.9 (0.1)
PLO POL	1.6 (0.1)	10.42 (0.03)
OOO	65.4 (0.9)	3.67 (0.03)
POO	8.6 (0.3)	2.7 (0.3)

TAGs present in less than 5% in both oils have been omitted. Numbers in parentheses correspond to the standard deviation of four measurements

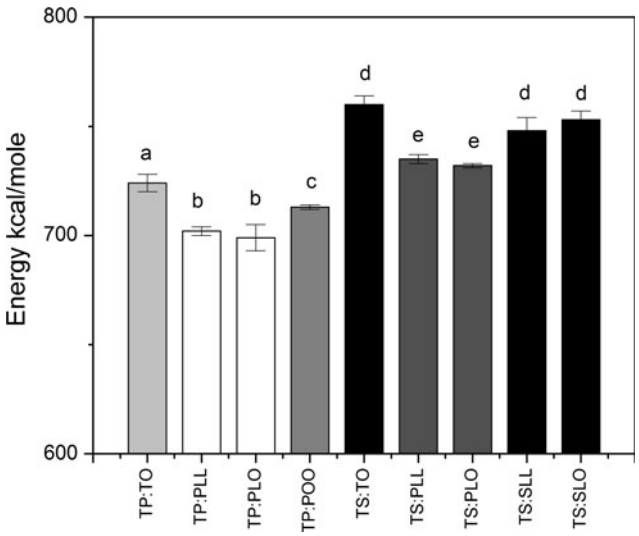

Fig. 4 Short range vdW interactions for different TAG mixes in a 1:1 M ratio. *Error bars* correspond to the standard deviation of 3–6 independent simulations with different starting configuration

747 ± 2 kcal/mol. This is an indication that vdW forces are somehow responsible for the liquid or solid behaviour of a TAG. Figure 4 shows the average vdW energy values for mixtures of TP:TO, TP:PLL, TP:PLO, TP:POO and the analogues in TS blends. PLL in our simulations is composed of one palmitic and two linoleic acid chains, PLO of one palmitic, one linoleic and one oleic acid chain and POO of one palmitic and two oleic acid chains. We have performed statistical analysis on our results to determine which mixes present a potential favorable vdW interaction. Also, different initial configurations of the same mix yield statistically equivalent results ($P > 0.05$). This then allowed for the calculation of an average value for different mixes and the determination of statistically significant differences between samples. The letters on the bars in Fig. 4 summarize our results. In this way, the TP:PLL, TP:PLO and TP:POO mixes have a significantly lower vdW energy than the TP:TO blend. A similar trend is seen for the TS:PLL and TS:PLO with respect to the TS:TO analogue. The same tendency was seen for mixtures in a 1:3 stoichiometry (data not shown). The last two bars correspond to blends of TS:SLL and TS:SLO. Although SLL and SLO exist in very small proportions in the oils, we have treated these blends with TS as "hypothetical". The purpose was to prove if the decrease in the vdW energy was related to the length of the TAGs involved or due to a specific effect related to the presence of palmitic acid in the TAG molecule. This last result seems to indicate that TAGs containing at least one saturated 16-carbon chain interact better with both TP and TS. Hence, the specificity does not arise from same length chains in the solute and solvent TAGs, but from a particular aspect of the palmitic acid.

Discussion

This work deals with the behavior of liquid oils in the presence of fully saturated TAGs. We have used both TP and TS with the purpose of comparing the effect that carbon chain length has on the behavior of the system. When a fluid has a preferential motion in a particular dimension or has an orientational restriction, it is said that the fluid is structured and hence displays anisotropy. This ordering of the fluid causes a change in the microviscosity of the system. Interestingly enough, this change in the microviscosity is highly correlated to the bulk viscosity of the system. Our fluorescence polarization results clearly indicate that there is a pre-nucleation structuring of the blend characterized by an increase of the anisotropy as a function of time as seen in Fig. 3. Our calorimetric data are supporting evidence that our FPS results are not due to a solubility or phase behavior effect, but rather a specific interaction of the blend components at the molecular level. In this work, we have ran single-component and bi-component MM simulations, to gain a better insight on the forces responsible for the pre-nucleation structuring seen in the FPS experiments.

The energies given by the Chem3D program are not related to any thermodynamic quantity, and have no meaning as absolute quantities. However, the values can be used for comparing relative behaviors between different conformations as done in this work. The total energy is divided into seven components: stretch, bend, stretch-bend combination, torsion, non-1,4 (or long range) van der Waals, 1,4 (or short range) van der Waals and dipole/dipole interactions. The sum of all these components corresponds to the total minimized energy of the system. Since bonded interactions are highly dependent on the

initial configuration of the molecule, we have only used the terms corresponding to non bonded interactions in our initial assessment of the energy minimization. The non-bonded interactions given by the program correspond to long and short range van der Waals forces and dipole/dipole interactions. Of these, only the short range vdW interactions displayed a pattern as a function of the TAG molecule used in the mix. This is in agreement with the work of Sato et al. [4] who have suggested that van der Waals interactions are responsible for the lamellar structure seen in their XRD measurements on monounsaturated TAGs.

For either TP or TS, Fig. 4 clearly indicates that the vdW energies are highest for mixes with TO. Hence the interaction between these TAGs is the least favorable. We believe that this is the reason why our FPS experiments show no increase in the anisotropy for the TO blends. Simulations for mixes of PLL and PLO with both saturated fats, show a decrease in the vdW energy with respect to the TO samples. We have interpreted this as an indication of a particular behavior occurring in the presence of TAGs that contain at least one palmitic acid. This explains the experimental result obtained through FPS, in which mixtures of TP:HOSfO and TP:SBO showed an increase in the microviscosity. HOSfO has about 10% of TAGs containing palmitic acid in their composition whereas SBO has a content of close to 30% of these TAGs. We believe that it is the presence and abundance of these palmitic acid-containing TAGs what determines the increase in the microviscosity prior to the actual nucleation of fat crystals. Hence, although an increase in anisotropy is seen in the TP:HOSfO blends, the highest effect is seen for the TP:SBO and TS:SBO samples.

Our results suggest that blends of saturated fats in oils that contain at least 10% of TAGs with at least one chain of palmitic acid, will show an increase in the microviscosity as a pre-nucleation step in the crystallization process. One could now hypothesize that this result is extensible to longer chain analogues. Hence, to induce crystallization one needs a liquid oil that has a relatively high content of TAGs that have at least one saturated chain. Interestingly, the effect is very specific to palmitic acid. The MM simulations performed on hypothetical blends of TS:SLL and TS:SLO indicate that the even if the saturated chain length is the same as that of the solid fat, the interaction is not necessarily favorable enough to induce ordering in the pre-nucleation stage. Very recently, Vereecken et al. [25] have suggested on the basis of DSC measurements, that TP seems to play a more important role as seeding agent in the crystallization of POP than TS does for SOS. This interesting conclusion agrees with the specific behavior seen for the palmitic-TAGs with respect to the stearic-containing analogues.

Conclusions

This work has studied the pre-nucleation ordering occurring in blends of saturated TAGs in different liquid oils. Our FPS experiments have given us insight on the microscopic level structuring that occurs at this stage. However, it was not clear which interactions were responsible for this effect at the molecular level. We performed MM simulations to address this aspect. MM is a fast and simple, yet powerful, tool that can provide complementary information to experimental data. Obviously, the results obtained need to be carefully interpreted based on the conditions used for the simulations. Once this is achieved, the resulting outcome of this procedure is usually a better understanding of the molecular interactions responsible for a particular phenomenon observed experimentally. Using MM we have been able to determine that van der Waals interactions are key in the stage prior to the nucleation of fats. We have also shown that a specific behavior occurs depending on the molecular composition of a particular TAG. These results indicate that both general and specific interactions play a role in the pre-nucleation step. It is our hope that this work has set grounds for the implementation of MM simulations in similar systems to the ones here presented.

References

1. Freedericksz V, Zolina V (1933) Forces causing the orientation of an anisotropic liquid. Trans Faraday Soc 29:919–930
2. Cebula DJ, McClements DJ, Povey MJW, Smith PR (1992) Neutron diffraction studies of liquid and crystalline trilaurin. J Am Oil Chem Soc 69:130–136
3. Larsson K (1972) Molecular arrangement in glycerides. Fette Seifen Anstrichmittel 74:136
4. Minato A, Ueno S, Smith K, Amemiya Y, Sato K (1997) Thermodynamic and kinetic study on phase behavior of binary mixtures of POP and PPO forming molecular compound systems. J Phys Chem B 101:3498–3505
5. Ueno S, Minato A, Yano J, Sato K (1999) Synchrotron radiation x-ray diffraction study of polymorphic crystallization of SOS from liquid phase. J Cryst Growth 198:1326–1329
6. Corkery RW, Rousseau D, Smith P, Pink DA, Hanna CB (2007) A case for discotic liquid crystals in molten triglycerides. Langmuir 23:7241–7246
7. Larsson K (1992) On the structure of the liquid state of triglycerides. J Am Oil Chem Soc 69:835–836
8. Hernqvist L (1984) On the structure of triglycerides in the liquid state and fat crystallization. Fette Seifen Anstrichmittel 86:297–300
9. Larsson K (1979) An x-ray scattering study of the L2-phase in monoglyceride-water system. J Colloid Interface Sci 72:152–153
10. Toro-Vazquez JF, Gallegos-Infante A (1996) Viscosity and its relationship to crystallization in a binary system of saturated triacylglycerides and sesame seed oil. J Am Oil Chem Soc 73:1237–1246
11. Marangoni AG (2002) Steady state fluorescence polarization spectroscopy as a tool to determine microviscosity and structural

order in lipid systems. In: Marangoni AG, Narine S (eds) Physical properties of lipids. Marcel Dekker, New York, pp 163–189
12. Murakami A, Nakaura M, Nakatsuji Y, Nagahara S, Tran-Cong Q, Makino K (1991) Fluorescent-labeled oligonucleotide probes: detection of hybrid formation in solution by fluorescence polarization spectroscopy. Nucleic Acids Res 19:4097
13. Parasassi T, De Stasio G, d'Ubaldo A, Gratton E (1990) Phase fluctuation in phospholipid membranes revealed by Laurdan fluorescence. Biophys J 57:1179–1186
14. Yguerabide J, Stryer L (1971) Fluorescence spectroscopy of an oriented model membrane. PNAS 68:1217–1221
15. Royer CA (1995) Fluorescence spectroscopy. Methods Mol Biol 40:65–89
16. Mann TL, Krull UJ (2003) Fluorescence polarization spectroscopy in protein analysis. Analyst 128:313–317
17. Nagarajan K, Myerson AS (2001) Molecular dynamics of nucleation and crystallization of polymers. Cryst Growth Des 1:131–142
18. Terrill NJ, Fairclough PA, Towns-Andrews E, Komanschek BU, Young RJ, Ryan AJ (1998) Density fluctuations: the nucleation event in isotactic polypropylene crystallization. Polymer 39:2381–2385
19. Perez-Martinez D, Alvarez-Salas C, Charo-Alonso M, Dibildox-Alvarado E, Toro-Vazquez JF (2007) The cooling rate effect on the microstructure and rheological properties of blends of cocoa butter with vegetable oils. Food Res Int 40:47–62
20. Kloek W, Walstra P, van Vliet T (2000) Crystallization kinetics of fully hydrogenated palm oil in sunflower oil mixtures. J Am Oil Chem Soc 77:389–398
21. Lakowicz JR (1999) Fluorescence anisotropy. In: Lakowicz JR (ed) Principles of fluorescence spectroscopy. Plenum Press, New York, pp 291–319
22. Allinger NL (1977) Conformational analysis. 130. MM2. A hydrocarbon force field utilizing V1 and V2 torsional terms. JACS 99:8127–8134
23. Weber G, Shinitzky M, Dianoux AC, Gitler C (1971) Microviscosity and order in the hydrocarbon region of micelles and membranes determined with fluorescent probes. I. Synthetic micelles. Biochemistry (NY) 10:2106–2113
24. Mateo CR, Lillo MP, Brochon JC, Martinez-Ripoll M, Sanz-Aparicio J, Acuna AU (1993) Rotational dynamics of 1,6-diphenyl-1,3,5-hexatriene and derivatives from fluorescence depolarization. J Phys Chem A 97:3486–3491
25. Vereecken J, Foubert I, Smith KW, Dewettinck K (2009) Effect of SatSatSat and SatOSat on crystallization of model fat blends. Eur J Lipid Sci Technol 111:243–258